JOURNAL OF CATALYSIS **172,** 64–75 (1997)
ARTICLE NO. CA971867

Effect of Catalyst Oxidation State and Structure on Thiophene Hydrodesulfurization over Model Molybdenum Catalysts

David L. Sullivan and John G. Ekerdt[1]

Department of Chemical Engineering, The University of Texas at Austin, Austin, Texas 78712

Received January 21, 1997; revised August 4, 1997; accepted August 14, 1997

Activity and product selectivity have been measured for thiophene hydrodesulfurization (HDS) over model silica-supported molybdenum catalysts at a pressure of 1 atm and at temperatures ranging from 398 to 673 K. The model catalysts feature isolated molybdenum atoms in the +2, +4, and +6 oxidation states and molybdenum dimers with each molybdenum atom in the +4 oxidation state. Silica-supported MoS_2, prepared by deposition and decomposition of $(NH_4)_2MoS_4$, was used for reference. There is a correlation between thiophene HDS activity and molybdenum oxidation state, with Mo(II) most active. Thiophene HDS activity does not show a significant structure dependence for isolated Mo(IV) versus dimeric Mo(IV) catalysts. Activation energies of 51.5 and 49.9 kJ/mol were determined for thiophene HDS over Mo(II) and MoS_2/SiO_2 catalysts, respectively. Butane and butenes are the major products of thiophene HDS with little butadiene detected. Activity and selectivity trends suggest the HDS reaction is initiated by η^1 binding of thiophene on the supported metal catalysts. © 1997 Academic Press

INTRODUCTION

Removal of sulfur from petroleum feedstocks is accomplished by hydrodesulfurization (HDS) in which the petroleum is treated with hydrogen over a $CoMo/Al_2O_3$ catalyst at temperatures from 575 to 725 K and pressures from 35 to 100 atm. The common industrial catalyst consists of alumina-supported molybdenum with a cobalt promoter. The catalyst is prepared by aqueous deposition of molybdenum and cobalt from $(NH_4)_6Mo_7O_{24}$ and $Co(NO_3)_2$, drying, and calcination in air at 825 K. The supported metal oxide is sulfided before use in H_2S/H_2 or in thiophene/H_2 at reaction conditions, to generate the active catalyst. Molybdenum is reduced during sulfidation, from Mo(VI) in MoO_3 to Mo(IV) in MoS_2. Formation of MoS_2 has been shown by many techniques including X-ray photoelectron spectroscopy (XPS), X-ray diffraction (XRD), extended X-ray absorption fine structure spectroscopy, and Raman spectroscopy. MoS_2 forms crystallites with a layered structure under these conditions (1). The active catalyst is a "Co–Mo–S" phase in which the cobalt atoms are located at the edges of MoS_2 sheets (2–5).

It has been proposed that HDS activity of unpromoted MoS_2/Al_2O_3 is due to exposed molybdenum atoms in a reduced oxidation state, which are formed at crystal edges and rims by loss of sulfur (6, 7). The remaining edge and rim sulfur is present as bridging sulfur or as terminal sulfhydryl groups (–SH). Sulfhydryl groups have been shown to be Bronsted acid sites (8) and are thought to be the source of hydrogen for hydrogenation and hydrogenolysis reactions that occur during HDS. The promoter effect is thought to be due to transfer of electron density from cobalt to molybdenum, further reducing the oxidation state of molybdenum (9, 10). However, the oxidation state and structure of the active site for reaction have not been clearly established. Spectroscopic and adsorption studies have been performed on unsupported and supported catalysts in an attempt to identify reduced molybdenum oxidation states and to relate oxidation state to HDS activity (2, 11). XPS (12, 13) and electron paramagnetic resonance spectroscopy (14–16) studies suggest the presence of Mo(III) on $CoMo/Al_2O_3$. Infrared study of chemisorbed CO on MoS_2/Al_2O_3 suggests formation of molybdenum sites in a low oxidation state (presumably +2) on the edges of MoS_2 platelets (17). However, the complexity of industrial catalysts has made definitive identification and quantification of the amount of molybdenum in reduced oxidation states difficult. In addition, the presence of a large amount of molybdenum in the +4 oxidation state (bulk MoS_2) with a relatively small amount of molybdenum in a reduced oxidation state makes it difficult to clearly determine the role of reduced oxidation states in HDS.

Several groups have used model systems such as Chevrel phases, single crystal metal surfaces, and organometallic complexes in an attempt to determine the effect of oxidation state on activity and to determine reaction mechanisms (11, 18, 19). Chevrel phases, with formal oxidation states ranging from +2.06 to +2.28, were much more active (per Mo atom) than MoS_2/Al_2O_3 (11, 20). Alumina-supported molybdenum disulfide can be prepared by deposition and

[1] Corresponding author. E-mail: ekerdt@che.utexas.edu.

0021-9517/97 $25.00

decomposition of $(NH_4)_2MoS_4$ (21). Thermal decomposition in helium produced MoS_x/Al_2O_3 with excess sulfur ($x > 2$). Reduction in hydrogen at 723 K resulted in loss of the excess sulfur and some stoichiometric sulfur ($x < 2$) producing exposed molybdenum atoms with an oxidation state less than +4. It was shown that activity for thiophene HDS correlated with the degree of thermal reduction of the MoS_x/Al_2O_3.

Thiophene is typically used as a model reactant because it is representative of the aromatic sulfur compounds that are difficult to desulfurize. Angelici has published a review of the structures and reactions of organometallic complexes containing thiophene ligands (19). Organometallic complexes are useful models in that they identify possible metal–adsorbate structures and the reaction of these structures. Thiophene in an η^1 (S-bound) coordination mode is a two-electron donor and occupies one coordination site of the metal atom. Thiophene in an η^4 coordination mode is a four-electron donor and requires two coordination sites. All organometallic complexes containing η^4-thiophene are due to the metal filling its 18 valence electrons with only four from thiophene. Thiophene in an η^5 coordination mode is a six-electron donor and requires three coordination sites. A thiophene bridging mode, with the sulfur atom coordinated to two metal atoms, has also been suggested as a possible reaction path (7, 22). Such a structure has not been seen in organometallic complexes. The most stable complexes are formed when the metal is in a low oxidation state (+2 or lower). The most reactive complexes are those with the weakest C–S bonds (η^5 coordination). While these complexes are useful for determining possible structures and reaction pathways, they do not provide a complete picture, since comparison of organometallic complexes to supported molybdenum disulfide is not straightforward and complexes containing molybdenum have yet to be synthesized. Silica-supported catalysts with metal atoms in discrete oxidation states, the approach employed herein, offer another method of modeling the industrial catalyst to explore the role of catalyst structure and oxidation state on thiophene HDS.

METHODS

All samples were prepared with Cab-O-Sil HS 5 silica (Cabot, 325 m^2/g) in a quartz U-tube that permitted sample preparation in an inert atmosphere and flow through reactions. Details of the preparation of silica-supported, isolated Mo(II) catalysts are described elsewhere (23–25). Approximately 0.5 g of silica was dehydrated under vacuum at 673 K for 1 h. $Mo(\eta^3\text{-}C_3H_5)_4$ was prepared in a method similar to that of Candlin and Thomas (26). The desired amount of $Mo(\eta^3\text{-}C_3H_5)_4$ was added to the silica at 273 K, whereupon reaction of the silica hydroxyls and some of the allyl ligands took place. The remaining allyl ligands were removed by reduction in hydrogen (Liquid Carbonic, 99.999%) at 773 K for 1 h.

Details of the preparation of silica-supported, dimeric Mo(IV) catalysts are presented elsewhere (27, 28). Approximately 0.5 g of silica was dehydrated under vacuum at 673 K for 1 h. The desired amount of $Cp_2Mo_2(CO)_6$ was added to the silica, whereupon reaction of the silica hydroxyls and the cyclopentadienyl ligands took place. The carbonyl ligands were removed in helium (UT Physics Dept., 99.99%) at 673 K.

Details of the preparation of silica-supported, isolated Mo(VI) catalysts are presented elsewhere (29–31). Mo(VI) catalysts with isolated metal atoms were prepared by oxidizing isolated Mo(II) or dimeric Mo(IV) catalysts in hydrocarbon-free air (Liquid Carbonic, hydrocarbons <0.5 ppm) at 823 K. Raman spectroscopy has shown that oxidation of isolated Mo(II) and dimeric Mo(IV) results in isolated Mo(VI) (31).

Details of the preparation of silica-supported, isolated Mo(IV) catalysts are presented elsewhere (32). Isolated Mo(IV) catalysts were prepared by photoreduction of isolated Mo(VI) in CO (Liquid Carbonic, 99.99%). The amount of isolated Mo(IV) formed was determined by the amount of CO_2 produced.

Silica-supported MoS_2 was prepared in a method similar to that of Vasudevan and Zhang for preparation of MoS_2/Al_2O_3 (21). Five grams of silica was added to a 20-ml aqueous solution of $(NH_4)_2MoS_4$ (0.572 g). The mixture was dried in vacuum at 295 K and stored under argon. XRD showed that the $(NH_4)_2MoS_4/SiO_2$ was amorphous. Approximately 200 mg of $(NH_4)_2MoS_4/SiO_2$ was used for each reaction and was transferred to the reaction U-tube under argon. Removal of the ammonia and excess sulfur was performed in flowing helium at 673 K for 1 h. MoS_2 crystals formed during the heating step (Fig. 1). The peak widths of the (100) and (110) reflections at 2θ of 32.7° and 58.3°, respectively, were used to determine the MoS_2 crystal size in the direction parallel to the basal planes (33). The peak widths of the (002) and (008) reflections at 2θ of 14.4° and 60.1°, respectively, were used to determine the MoS_2 crystal size in the direction perpendicular to the basal planes. Estimated average dimensions for the silica-supported MoS_2 crystallites are 134 Å in the directions parallel to the basal planes and 48 Å in the direction perpendicular to the basal planes. The MoS_2 crystallites contain approximately 10% of the molybdenum at perimeter sites. Bulk MoS_2 (Aldrich, 99%) measured under the same conditions had peak widths of 0.36° to 0.60° 2θ for the same reflections showing that instrumental peak broadening was small compared to that due to the crystallites. XPS of MoS_2/SiO_2 following the heating step to 673 K showed binding energies for Mo $3d_{3/2}$ at 231.4 eV, Mo $3d_{5/2}$ at 228.2 eV, and for S 2*p* at 161.4 eV. The relative sensitivity of the XPS for Mo 3*d* and S 2*p* peaks was empirically determined by measurement of bulk MoS_2

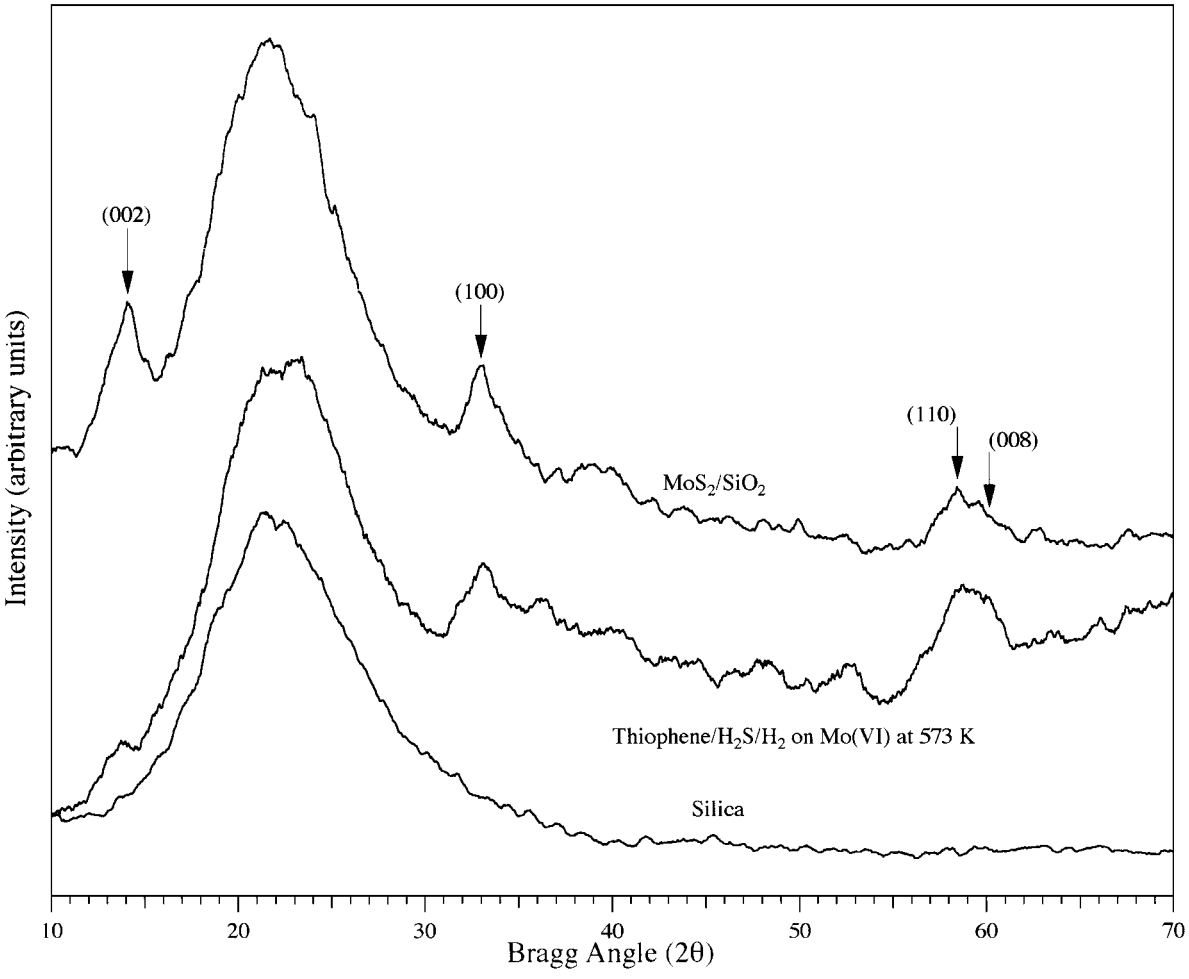

FIG. 1. XRD of blank silica, Mo(VI) catalyst after reaction of thiophene/H_2S/H_2 at 573 K and MoS_2/SiO_2 after heating to 673 K.

under identical conditions and agreed well with reported values (34). Peak areas of MoS_2/SiO_2, corrected for relative sensitivity, indicate a S/Mo ratio of 2.07.

Atomic absorption spectroscopy was used to determine molybdenum content of the samples (28). The Mo(II), isolated Mo(IV), dimeric Mo(IV), and Mo(VI) catalysts do not form crystallites during preparation, so all the molybdenum atoms are available for reaction.

Powder X-ray diffraction was performed with a Philips PW 1729 X-ray generator using Cu Kα X-rays ($\lambda = 1.54$ Å) at 40 kV and 40 mA. A Philips APD 3520 was used to integrate intensity (counts) with a step size of 0.05° 2θ and a scan speed of 1.5° 2θ/min.

X-ray photoelectron spectra were collected on a Physical Electronics system with monochromatic Al Kα X-rays (1486.7 eV) with a source power of 300 W. Chamber pressure during measurement was on the order of 10^{-9} Torr. Samples were transferred from the reaction U-tube to the XPS chamber under an inert atmosphere by use of a dry box and air-tight sample transfer case. Samples were mounted by pressing the powder onto indium foil or double-sided tape. A neutralizer was used to minimize charging of the powder during data collection. Survey scans were collected from 0–1400 eV with a step size of 0.40 eV, for 200 ms/step, with a pass-energy of 94 eV. High resolution scans were taken in the Mo 3*d* region (220–245 eV) and in the Si 2*s* and S 2*p* region (145–170 eV). High resolution scans were collected with a step size of 0.10 eV, for 650 ms/step, with a pass-energy of 24 eV. Binding energies were corrected for the small amount of sample charging by translating the data so that the Si 2*s* and Si 2*p* peaks were at 155.0 and 103.5 eV, respectively (34). Spectra were fit with Gaussian peaks using a Levenberg–Marquardt error-minimization routine. In fitting a spectrum, either a single molybdenum oxidation state was considered or multiple oxidation states were considered. Binding energies, peak heights, and peak widths were allowed to vary when fitting a spectrum to a single oxidation state. Fitting of a spectrum for multiple oxidation states was performed with the Mo $3d_{5/2}$ and Mo $3d_{3/2}$ peaks at a fixed separation of 3.1 eV and with a fixed area ratio of 6/4. None of the fits indicated the presence of multiple molybdenum oxidation states.

Thiophene (Janssen, 99+%) was purified by several freeze/pump/thaw cycles before use. Gas chromatography confirmed that impurities were less than 0.25%. Major impurities were methanethiol (0.1%), ethanethiol (0.03%), propanethiol (0.01%), and butanethiol (0.04%). The thiophene contained no detectable tetrahydrothiophene or dihydrothiophene. Thiophene was added to the samples by hydrogen flow at 8.0 ml/min through a saturator containing liquid thiophene at 295 K and 1 atm. This arrangement resulted in 8.7% thiophene in hydrogen.

The effluent from the reaction U-tube was sampled on-line with a Hewlett–Packard 5890 gas chromatograph equipped with a flame ionization detector. A 1-ml sample from an automatic sampling valve was injected onto a 50 m × 0.53 mm PLOT Al_2O_3/KCl column (Chrompak). The detector was calibrated with a 1010 ppm CH_4/1010 ppm C_3H_8/He mixture (Matheson, certified). A mixture of methane, ethane, propane, propene, *i*-butane, *n*-butane, *t*-2-butene, 1-butene, *i*-butane, *c*-2-butane, and butadiene in helium (in-house) was used to calibrate retention times. Hydrogen sulfide formation was measured using a Hewlett–Packard 5880 gas chromatograph, with a Porapak Q column and a thermal conductivity detector. Hydrogen sulfide was detected during thiophene HDS over all the catalysts but was not quantified due to poor sensitivity and hydrocarbon interferences.

Conversions of thiophene were less than 4%, except for the Mo(II) catalysts at 673 K, which had 17% conversion. Cab-O-Sil HS 5 is a nonporous support so the entire surface area is accessible to reactant molecules. The number of active sites used to calculate turnover frequencies (TOFs) (moles reacted/mole metal-sec) and turnover numbers (TONs) (total moles reacted/mole metal) for Mo(II), dimeric Mo(IV), and Mo(VI) catalysts is the number of metal atoms on the catalyst. TOFs and TONs for isolated Mo(IV) catalysts were based on the amount of isolated Mo(IV) formed during photoreduction. The amount of reaction due to the isolated Mo(IV) was calculated by subtracting the amount of reaction due to unreduced Mo(VI) from the total reaction for the sample. TOFs and TONs for MoS_2/SiO_2 catalysts were based on the estimated number of perimeter molybdenum atoms (10% of the total molybdenum).

RESULTS

Figure 2 shows a plot of thiophene HDS versus time for Mo(II) at 573 K. All samples for thiophene/H_2 reaction showed a similar steady state with no change in activity or selectivity with time. Samples were run for long times to establish that the reaction is catalytic. TONs for thiophene HDS over Mo(II), isolated Mo(IV), dimeric Mo(IV), and MoS_2/SiO_2 catalysts of 193, 2.5, 27, and 46, respectively, were obtained for the longest runs.

XRD was used to determine whether MoS_2 crystallites were formed by sulfidation of the Mo(II), isolated Mo(IV), dimeric Mo(IV), or Mo(VI) catalysts. None of the catalysts formed MoS_2 during reaction of thiophene/H_2, even

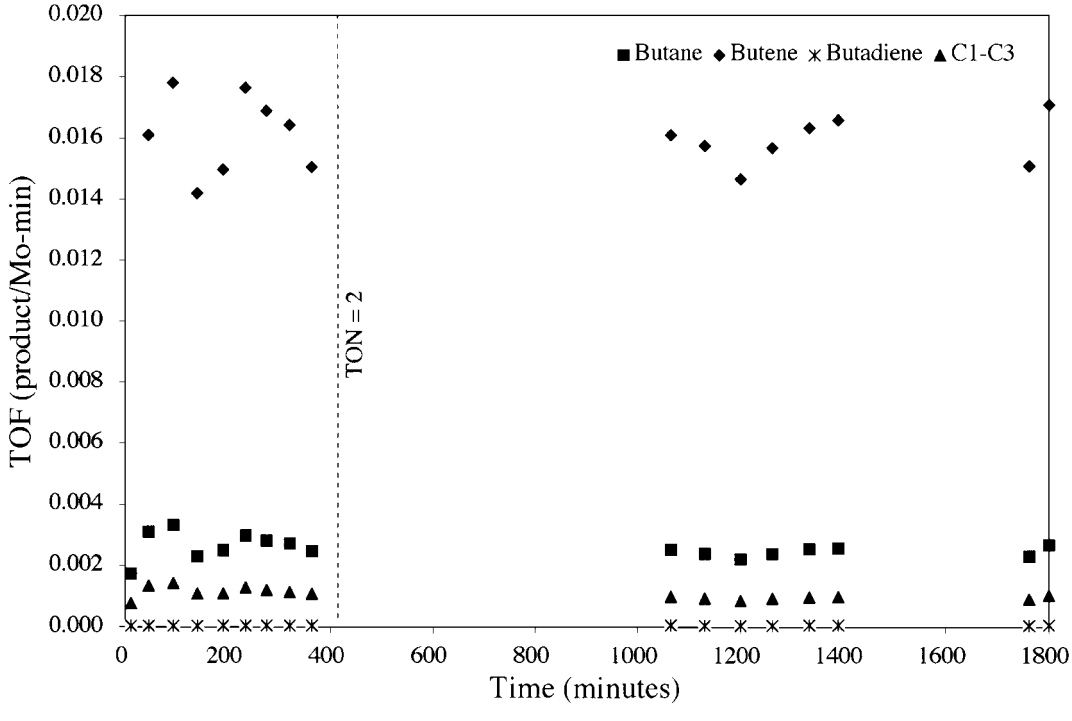

FIG. 2. Thiophene HDS products versus time for Mo(II) catalyst at 573 K.

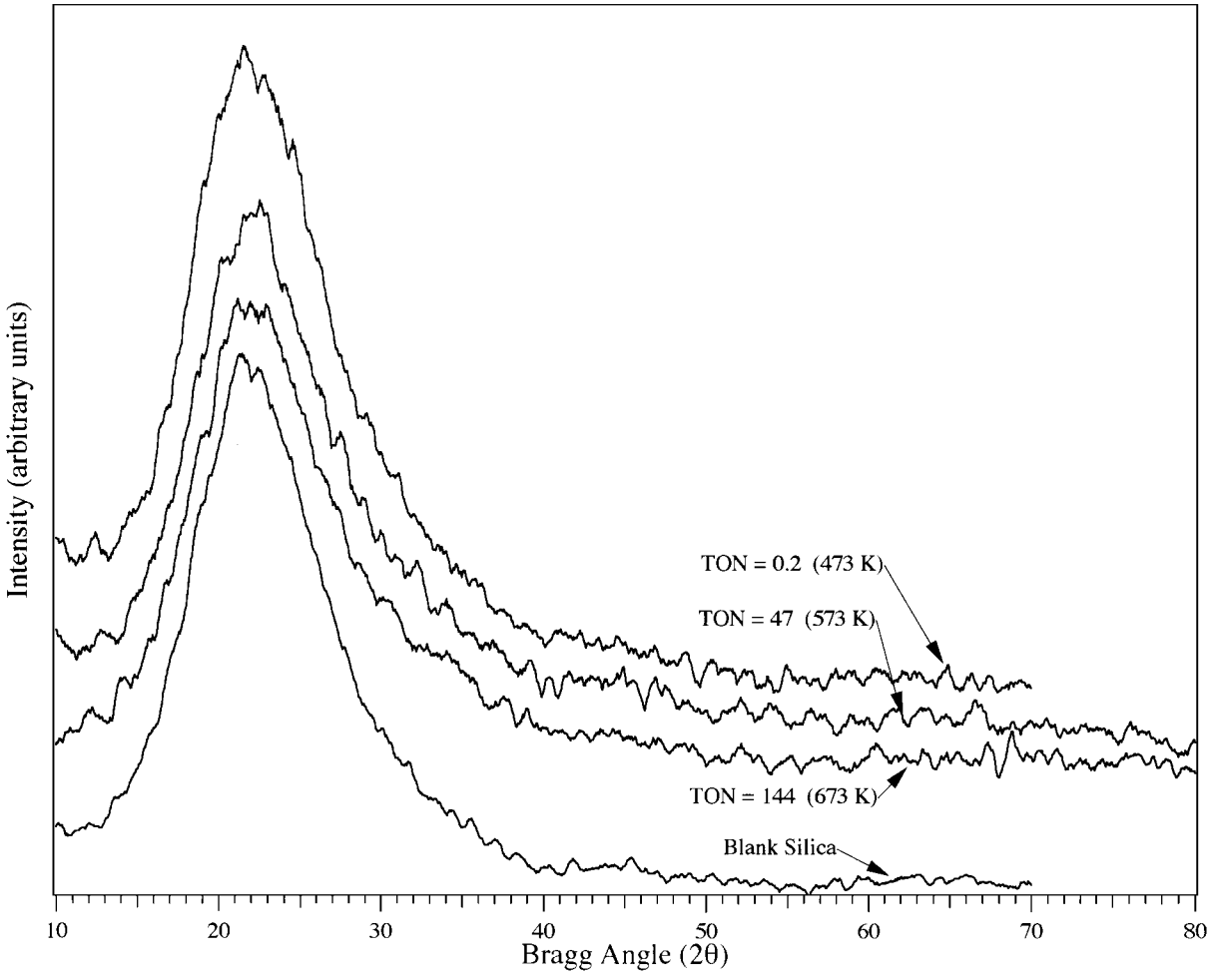

FIG. 3. XRD of Mo(II) catalysts after thiophene HDS.

at high temperatures and high TONs (Fig. 3). Attempts to sulfide Mo(II), by reaction with 1087 ppm H_2S/H_2 (Matheson, certified) at 773 K, did not result in formation of MoS_2. MoS_2 could only be formed from Mo(VI) by reaction of thiophene/H_2S/H_2 at 573 K (Fig. 1).

XPS was used to determine whether the catalysts changed oxidation state during thiophene HDS and to determine whether the catalysts were becoming sulfided on a scale smaller than observable by XRD. Table 1 summarizes the XPS results. In all spectra, the binding energy of

TABLE 1

XPS Binding Energies of Molybdenum and Sulfur for Unused and Used Catalysts[a]

Catalyst	Reactants	Temperature (K)	Mo $3d_{3/2}$			Mo $3d_{5/2}$			S 2*p*
			B.E. (eV)	FWHH (eV)	Area (%)	B.E. (eV)	FWHH (eV)	Area (%)	B.E. (eV)
Mo(II)	—	—	231.7	3.4	37	228.5	3.9	63	—
Mo(II)	Thiophene/H_2	673	231.6	4.0	39	228.6	4.5	61	—
Mo(II)	Thiophene/H_2S/H_2	573	231.8	3.4	36	228.3	3.8	64	—
Dimeric Mo(IV)	—	—	234.8	4.6	38	231.7	5.1	62	—
Dimeric Mo(IV)	Thiophene/H_2	473	235.2	6.0	41	231.9	6.5	59	—
Mo(VI)	—	—	237.2	3.8	40	233.8	3.7	60	—
Mo(VI)	Thiophene/H_2	473	236.6	4.7	37	233.8	4.3	63	—
Mo(VI)	Thiophene/H_2S/H_2	573	231.3	4.4	41	228.3	4.0	59	161.5
MoS_2/SiO_2	—	—	231.4	1.9	43	228.2	1.6	57	161.4

[a] B.E., binding energy; FWHH, peak width at half height.

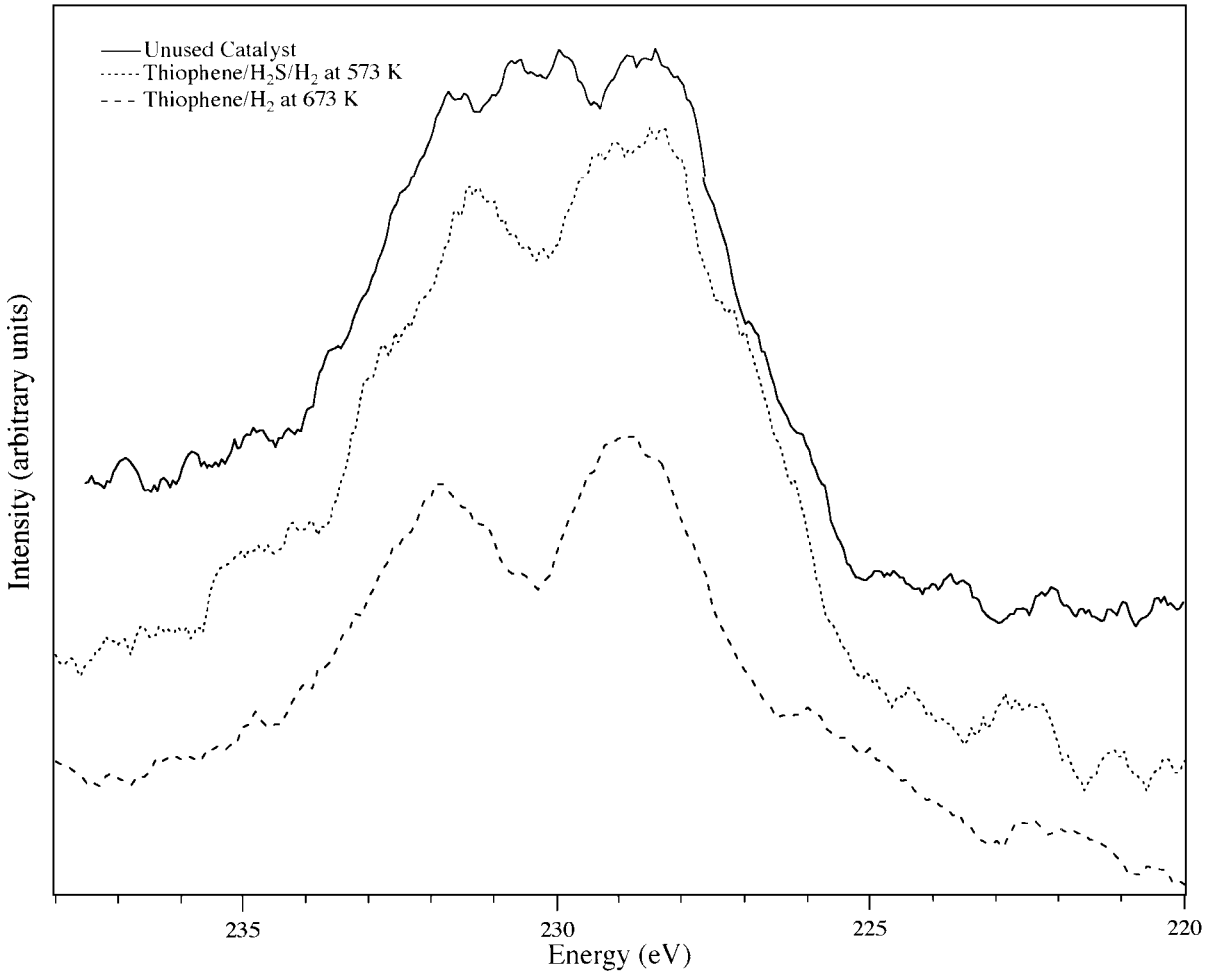

FIG. 4. Molybdenum XPS of Mo(II) catalysts.

Mo $3d_{3/2}$ is about 3.1 eV higher than the binding energy of Mo $3d_{5/2}$. Fitting of the spectra gives Mo $3d_{5/2}$ and Mo $3d_{3/2}$ peak areas which are close to the theoretical ratio of 6/4.

Figure 4 shows representative spectra in the region of Mo 3*d* binding energy for Mo(II) catalysts. The spectrum of unused Mo(II) has a Mo $3d_{5/2}$ binding energy of 228.5 eV. The spectrum of Mo(II) after reaction with thiophene/H_2 at 673 K has a Mo $3d_{5/2}$ binding energy of 228.6 eV. The spectrum of Mo(II) after reaction with thiophene/H_2S/H_2 at 573 K has a Mo $3d_{5/2}$ binding energy of 228.4 eV. The Mo $3d_{5/2}$ peaks for all three samples agree with the 228.4 eV assigned to Mo(II) (25). Figure 5 shows representative spectra in the region of Si 2*s* and S 2*p* binding energies for Mo(II) catalysts and MoS_2/SiO_2. The peak at 155.0 eV in all the spectra is Si 2*s* due to the silica support. The peak at 161.2 eV of the MoS_2/SiO_2 spectrum is S 2*p* (34). The used Mo(II) catalysts do not show a S 2*p* peak.

Figure 6 shows representative spectra in the region of Mo 3*d* binding energy for dimeric Mo(IV) catalysts and the fit of the unused dimeric Mo(IV). Fitting of all spectra were performed in the same manner but are not shown for clarity. XPS of unused dimeric Mo(IV) and of dimeric Mo(IV) after reaction with thiophene/H_2 at 473 K shows Mo $3d_{5/2}$ binding energies of 231.7 eV and 231.9 eV, respectively. Used dimeric Mo(IV) catalysts do not show a S 2*p* peak.

Figure 7 shows representative spectra in the region of Mo 3*d* binding energy for Mo(VI) catalysts and MoS_2/SiO_2. XPS of unused Mo(VI) shows a Mo $3d_{5/2}$ binding energy of 233.8 eV. XPS of Mo(VI) after reaction with thiophene/H_2 at 473 K shows a Mo $3d_{5/2}$ binding energy of 233.9 eV and no S 2*p* peak. XPS results (not shown) reveal that Mo(VI) does not change during reaction with thiophene/H_2S/H_2 at 473 K. XPS of Mo(VI) after reaction with thiophene/H_2S/H_2 at 573 K has binding energies for Mo $3d_{5/2}$ of 228.3 eV and for S 2*p* of 161.5 eV, which agree with the data for MoS_2/SiO_2 and indicates (along with XRD) that MoS_2 was formed. The S/Mo ratio was only 0.82 following thiophene/H_2S/H_2 reaction at 573 K for 100 h, suggesting that not all the Mo(VI) transformed to MoS_2. XPS results (not shown) reveal that Mo(VI) forms MoS_2 crystallites during reaction

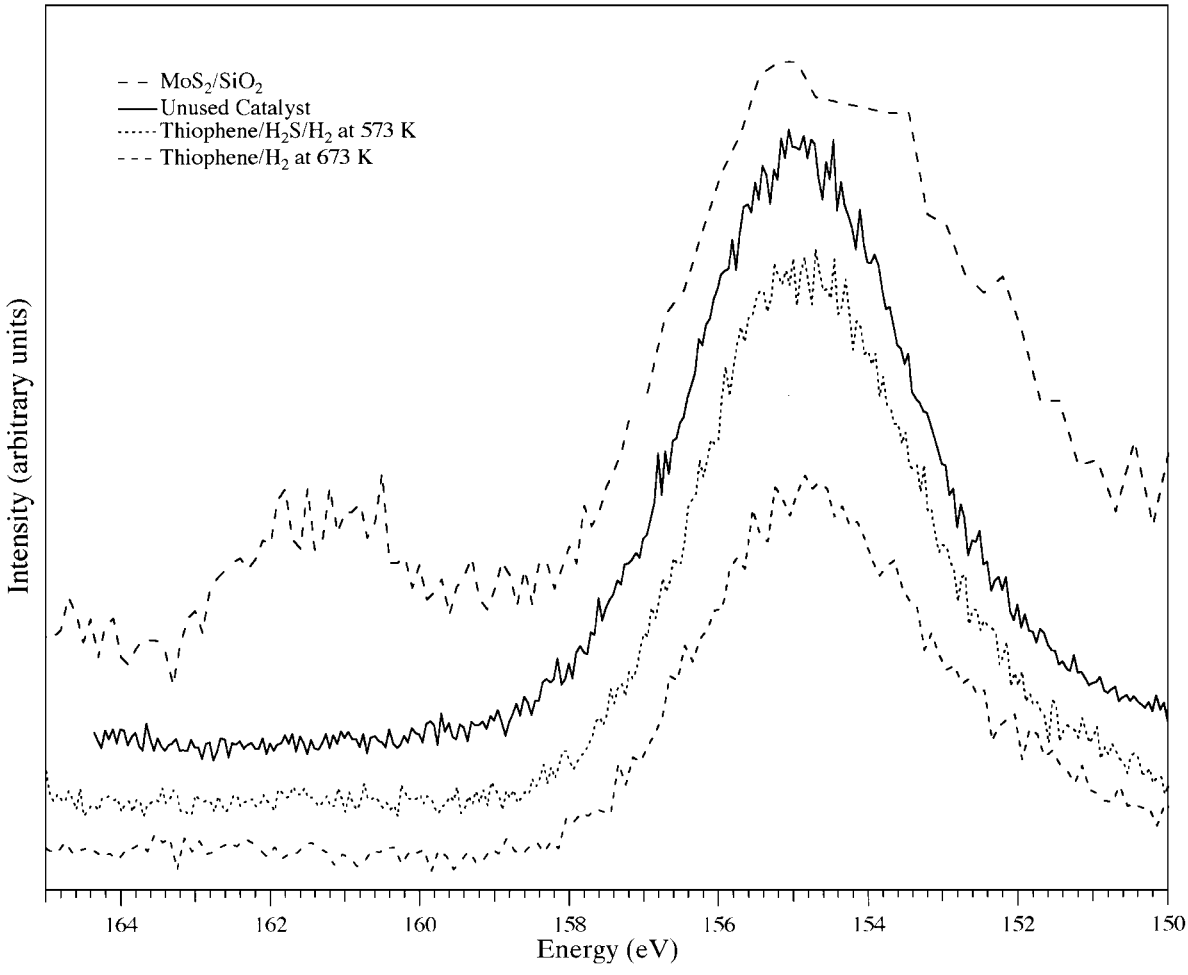

FIG. 5. Sulfur XPS of Mo(II) catalysts and MoS_2/SiO_2.

with thiophene/H_2 at 573 K. Since Mo(II), dimeric Mo(IV), and Mo(VI) catalysts do not change oxidation state or become sulfided during thiophene HDS at 473 K, it is reasonable to assume that isolated Mo(IV) does not change oxidation state or become sulfided during thiophene HDS at 473 K.

Table 2 presents steady state reaction rates and Fig. 8 shows steady state product distributions observed for thiophene HDS over Mo(II), isolated Mo(IV), dimeric Mo(IV), and MoS_2/SiO_2 catalysts at 473 K. Thiophene HDS rates over Mo(II) are approximately a factor of two lower than rates reported for similarly prepared Mo(II) catalysts (35, 36). The temperature of 473 K was chosen for most of the experiments to be high enough so that reaction was not limited by product desorption but low enough so that hydrogenation of butene and butadiene were avoided. Mo(II) catalysts had the highest reaction rate for dispersed cations. Isolated Mo(IV) and dimeric Mo(IV) had similar reaction rates. All the catalysts showed similar product distributions. Butenes were the major product over all catalysts. Butane and light products (C_1–C_3) were formed in small amounts over all the catalysts, except for dimeric Mo(IV) which showed a large amount of butane. Butadiene was a very minor product over all the catalysts, except for isolated Mo(IV) which had a significant amount. Figure 9 shows products of thiophene HDS over Mo(II) for temperatures from 398 to 672 K. The product distributions show some increase in butane at higher temperatures

TABLE 2

Thiophene HDS Rates at 473 K

Catalyst	Rate (Thiophene/Mo-s × 10^6)
Mo(II)	56
Isolated Mo(IV)	28
Dimeric Mo(IV)	26
Mo(VI)	2
MoS_2/SiO_2	215

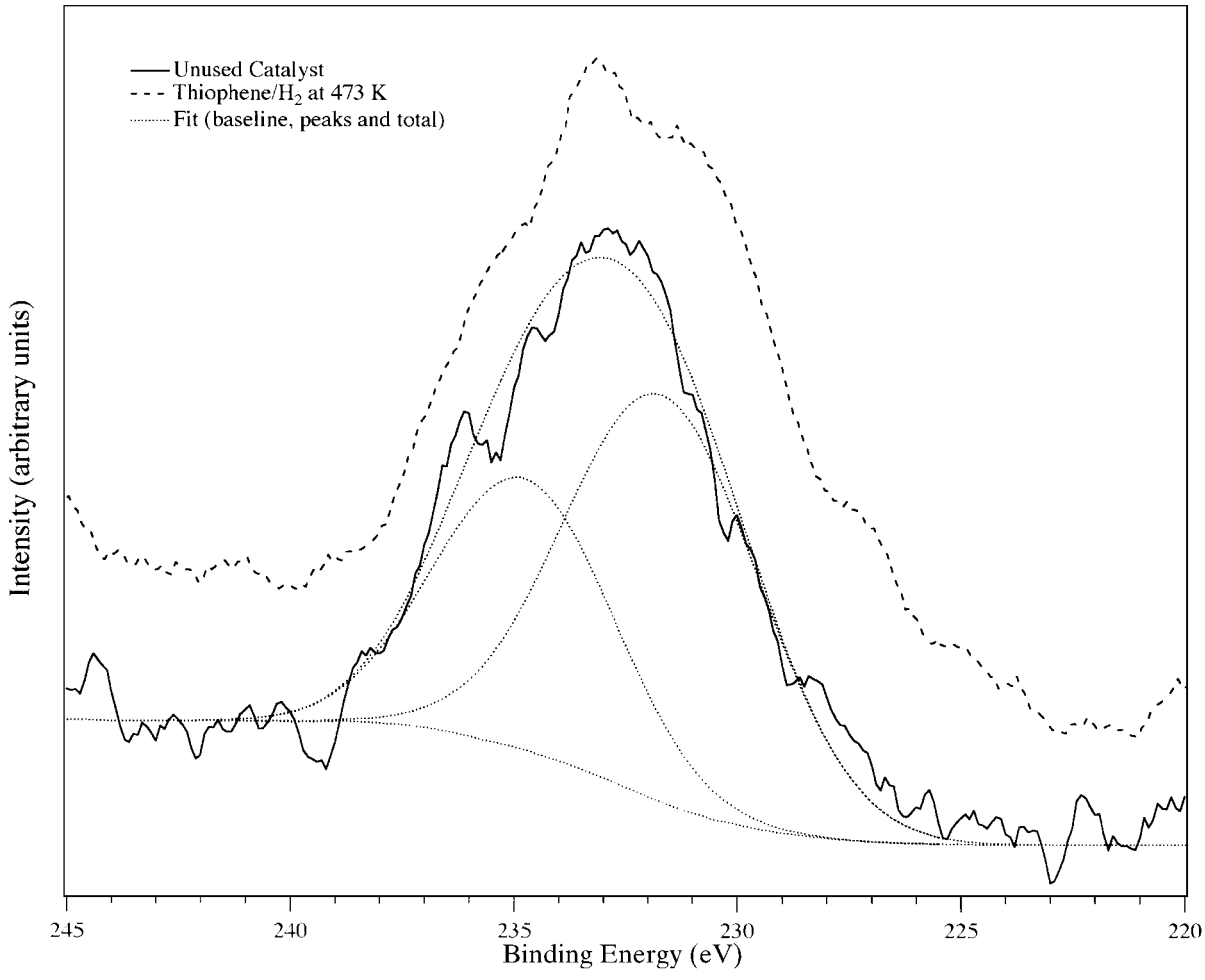

FIG. 6. Molybdenum XPS of dimeric Mo(IV) catalysts and fitting of dimeric Mo(IV).

but, the major product is butene at all temperatures. Butadiene is only significant at 398 K. Figure 10 shows an Arrhenius plot for Mo(II) and MoS_2/SiO_2 catalysts. Apparent activation energies for thiophene HDS over Mo(II) and MoS_2/SiO_2 catalysts were 51.5 ± 3.4 and 49.9 ± 6.7 kJ/mol, respectively. Reactions of butenes and butadiene in H_2 were performed to determine whether these reactions might occur after desulfurization of thiophene. Butenes and butadiene were fed at concentrations of roughly 1000 ppm to approximate the concentration during thiophene HDS. Products from hydrogenation of 1-butene, *t*-2-butene, and butadiene are presented in Tables 3 and 4. Isomerization

TABLE 3

Products of Hydrogenation of Butenes

Reactant	Catalyst	Temperature (K)	Products (mole percent)						
			C_1–C_3	C_4H_{10}	1-C_4H_8	*c*-2-C_4H_8	*t*-2-C_4H_8	*i*-C_4H_8	C_4H_6
1-C_4H_8	Mo(II)	470	0.01	0.35	43	31	23	2.2	0.02
1-C_4H_8	Mo(VI)	470	0.06	0.90	60	24	15	0	0.14
1-C_4H_8	MoS_2/SiO_2	470	0.03	0.23	97	2.1	0.50	0	0.05
t-2-C_4H_8	Mo(II)	380	1.1	0.60	0	28	67	1.2	2.7
t-2-C_4H_8	Mo(II)	460	3.3	23	19	22	29	3.8	1.2
t-2-C_4H_8	Mo(II)	480	2.4	97	0	0.12	0.30	0	0
t-2-C_4H_8	Mo(II)	550	5.4	94	0	0.09	0.25	0	0.34

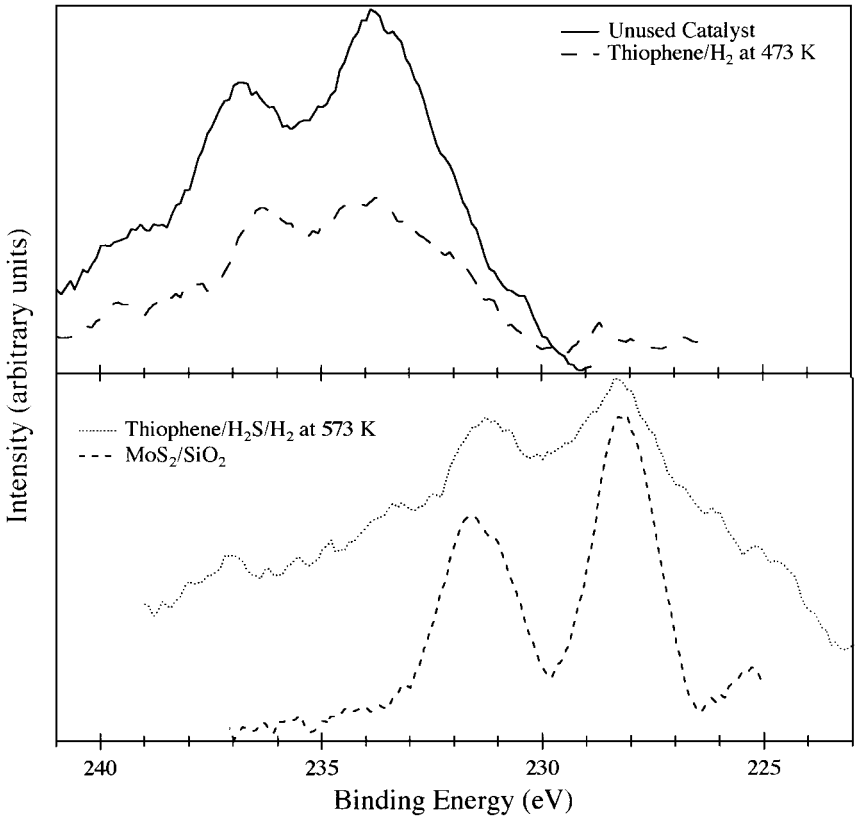

FIG. 7. Molybdenum XPS of Mo(VI) catalysts and MoS_2/SiO_2.

dominates butene reaction below about 475 K with hydrogenation to butane becoming dominant above about 475 K. Butadiene hydrogenation to butene and butane is shown to be facile.

DISCUSSION

The results lead us to conclude that the oxidation state and structure of the Mo(II), isolated Mo(IV), and dimeric

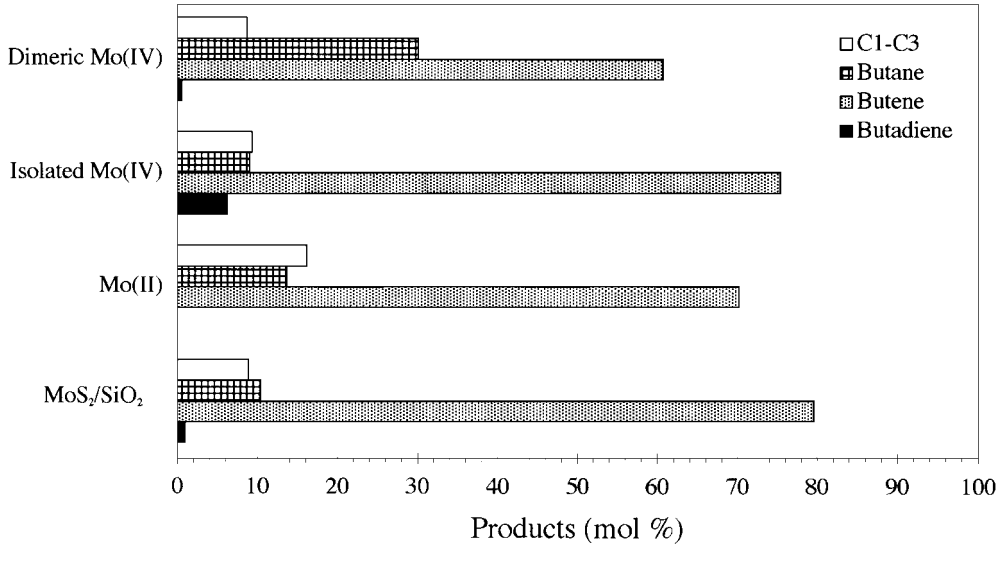

FIG. 8. Thiophene HDS products at 473 K for Mo(II), isolated Mo(IV), dimeric Mo(IV), and MoS_2/SiO_2 catalysts.

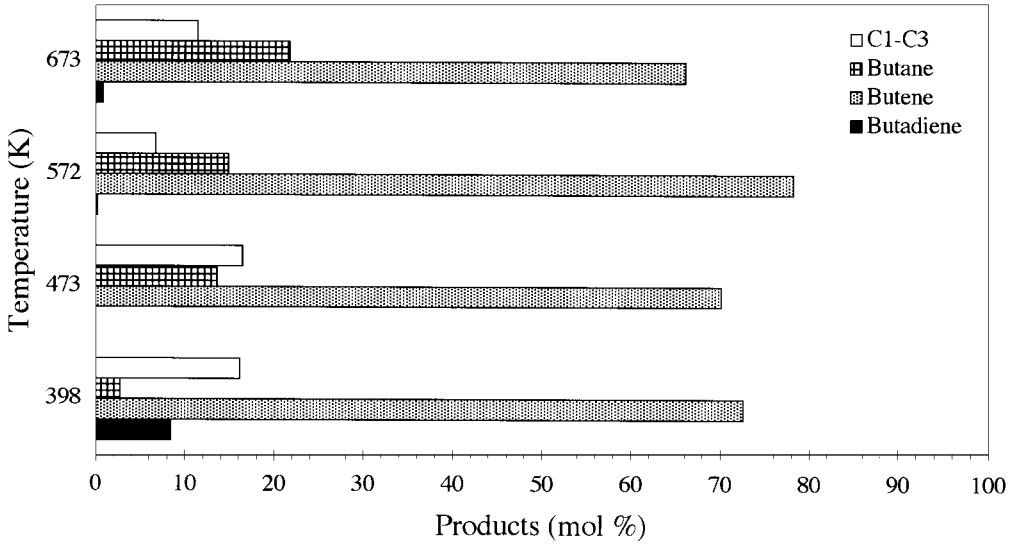

FIG. 9. Thiophene HDS products for Mo(II) catalysts at temperatures of 398 to 673 K.

Mo(IV) catalysts are not changing during thiophene HDS. First, XRD does not show formation of MoS_2 crystallites. Second, if the catalyst structures were changing during thiophene HDS, we would expect to see a change in TOF to the value found for MoS_2/SiO_2. Sulfidation of the Mo(II), isolated Mo(IV), dimeric Mo(IV), or Mo(VI) catalysts should result in a dramatic increase in TOF. Only in the reaction of thiophene over Mo(VI) at 573 K is there a change in TOF with time. For these samples, XRD and XPS results show that MoS_2 was formed. Formation of MoS_2 from Mo(VI) was expected to occur since the industrial catalysts are formed by sulfidation of fully oxidized molybdenum. For reaction of thiophene/H_2 over Mo(II), isolated Mo(IV), dimeric Mo(IV), and Mo(VI) catalysts, steady state is achieved with no significant change in TOF or product distribution with increasing reaction time. Third, XRD and XPS results show that attempts to sulfide Mo(II) catalysts by reaction with H_2S/H_2 at 773 K did not produce MoS_2. Finally, the XPS results show that the oxidation states of the Mo(II) and Mo(IV), catalysts do not change and the samples do not become sulfided during thiophene/H_2 reaction. Therefore, we are observing thiophene HDS over the model catalyst structures described.

Table 2 shows that Mo(II) catalysts are the most active (among dispersed catalysts) for thiophene HDS, which is consistent with the results obtained for thiophene HDS by Chevrel phases and thermally reduced MoS_2/Al_2O_3. Our data add more support to the argument that the active sites

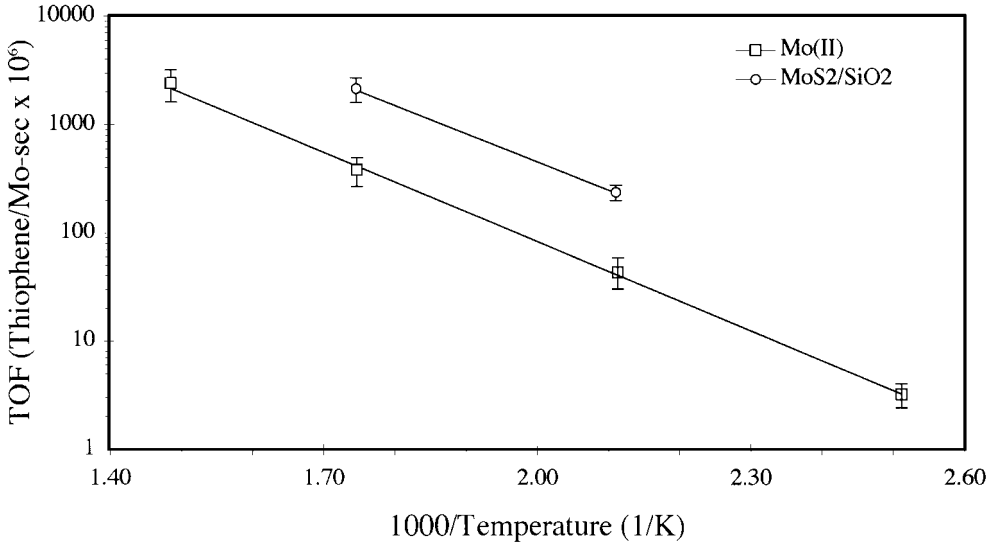

FIG. 10. Thiophene HDS rates versus temperature for Mo(II) and MoS_2/SiO_2 catalysts.

TABLE 4

Products of Hydrogenation of Butadiene

Reactant	Catalyst	Temperature (K)	Products (mole percent)			
			C_1–C_3	C_4H_{10}	C_4H_8	C_4H_6
C_4H_6	Mo(II)	470	0	20	5.4	75
C_4H_6	Mo(II)	550	3.7	45	20	31
C_4H_6	Mo(II)	650	17	44	18	22

for HDS are reduced molybdenum atoms, which on MoS_2 crystallites are the sites with sulfur vacancies.

The edges of a MoS_2 slab contain two distinct molybdenum environments, which may be active sites after removal of sulfur (7, 24). The $10\bar{1}0$ face has terminal sulfur atoms, which are bound to only one molybdenum atom. The $\bar{1}010$ face has bridging sulfur atoms, which are bonded to two molybdenum atoms. The comparable activity of isolated Mo(IV) and dimeric Mo(IV) for thiophene HDS suggests that adsorption at a site containing two molybdenum atoms is not a requirement for HDS and does not enhance the HDS rate. The increased amount of butane observed over dimeric Mo(IV) catalysts suggests that they are better hydrogenation sites than isolated Mo(IV) sites. We believe that this is due to the dimers favoring hydrogenolysis of butanethiolate to butane, instead of hydrogen elimination to butene. This agrees with the observation that hydrogenation is easier on the $\bar{1}010$ face than on the $10\bar{1}0$ face (22). However, the increased hydrogenation of butanethiolate does not effect the overall thiophene HDS rate significantly. The rate of butanethiol HDS is about 15 times faster than the rate of thiophene HDS (37).

Thiophene HDS by isolated Mo(IV), which can only coordinate a two-electron donor molecule, shows that η^5-thiophene adsorption is not required for HDS. Thiophene could adsorb on Mo(II) in an η^4 or η^1 mode but could only adsorb on isolated Mo(IV) in an η^1 mode. An interesting possibility for Mo(II) is η^1-adsorption of thiophene with the hydrogen for reaction adsorbed on the same metal atom. Similarly, thiophene HDS over dimeric Mo(IV) could occur by η^1-adsorption of thiophene on one metal atom of the dimer with the hydrogen for reaction adsorbed on the other metal atom. However, if the same mechanism is occurring over Mo(II), isolated Mo(IV), and dimeric Mo(IV) then the only possibility is η^1-adsorption of thiophene. Hydrogen for hydrogenation and hydrogenolysis reactions on the dispersed catalysts may come from neighboring hydroxyl groups; similar to what it thought to occur with sulfhydryl groups on MoS_2 catalysts.

Apparent activation energies for thiophene HDS over Mo(II) and MoS_2/SiO_2 are comparable to some values reported for supported MoS_2 (3, 38, 39). Activation energies between 57 and 105 kJ/mol have been measured for thiophene HDS over supported MoS_2. A number of possible reaction sites and possible isomerization, hydrogenation, and hydrogenolysis reactions may occur on the different catalysts; these sites and competing reactions will factor into the apparent activation energy and may explain the range of activation energies. The agreement that we find for Mo(II) and MoS_2/SiO_2 suggests that the same rate limiting step in the HDS reaction mechanism is occurring over both catalysts. Since the activation energies are similar, some of the difference in TOFs for thiophene HDS over Mo(II) and MoS_2/SiO_2 could be due to a difference in the preexponential factors, in a way not revealed in these studies. It is believed that the rate limiting step is the initial hydrogenation of thiophene (19). The difference in TOFs may also be due to different amounts of hydrogen available for reaction. There may be more sulfhydryl groups on the MoS_2/SiO_2 surface than there are hydroxyl groups on the dispersed molybdenum catalysts. Alternatively, sulfhydryl groups could be more reactive than hydroxyl groups, due to the difference in bond energies between S–H (338 kJ/mol) and O–H (463 kJ/mol) bonds (40).

The similarity of product distributions of thiophene HDS over the different catalysts (Fig. 8) suggests that the same mechanism is occurring over all the catalysts studied. The rate limiting reaction step is not necessarily the reaction step that controls selectivity. It has been proposed that butadiene is the primary desulfurization product and undergoes hydrogenation and isomerization to butene and butane (10, 18, 19). The low amount of butadiene produced suggests that it is not a primary desulfurization product. However, hydrogenation of butadiene has been shown, by us and by other investigators (38, 41), to be very fast. It has been shown that the rate of hydrogenation of 1-butene to butane over $CoMo/Al_2O_3$ catalysts is negligible but that 1-butene readily isomerizes to a mixture of butenes (38, 41, 42). We have shown that butene readily isomerizes at temperatures below about 475 K and that butene is easily hydrogenated to butane above about 475 K. Figure 9 shows an increasing amount of butane with increasing temperature, suggesting that some hydrogenation of butenes is occurring following desulfurization. However, based on the results in Table 3, we would expect very little butene in the products of thiophene HDS at temperatures above 470 K. That butenes are observed suggests that only a few sites are performing hydrogenation and isomerization of butene and butadiene during thiophene HDS. This could be due to a competition between thiophene, butadiene, butene, butane, and hydrogen sulfide for vacant metal sites. Preferential adsorption of thiophene and hydrogen sulfide on the active sites (22, 38, 43) inhibits isomerization and hydrogenation of butene and butadiene.

Light products may be produced during thiophene HDS by decomposition of butadiene (Table 4). However, the small amount of butadiene produced during thiophene

HDS suggests that this is not a significant route. Light products are probably produced by nonselective decomposition of thiophene in a manner similar to that on single crystal metals (18).

In summary, we have shown that isolated Mo(II), isolated Mo(IV), and dimeric Mo(IV) catalysts did not change oxidation state or become sulfided during thiophene HDS. The activity of isolated Mo(IV) catalysts suggests that HDS of thiophene occurs through η^1 adsorption. Mo(II) catalysts were the most active, of the dispersed catalysts, for thiophene HDS. The higher activity of thiophene HDS over MoS_2/SiO_2 catalysts than over Mo(II) catalysts could be due to differences in reactivity of sulfhydryl and hydroxyl groups.

ACKNOWLEDGMENTS

This work was supported by the U.S. Department of Energy, Office of Basic Energy Sciences under Grant DE-FG03-95ER14570. We gratefully acknowledge the assistance of Sandra Whaley and Deborah Hess of the Department of Chemistry and Biochemistry for assistance with the XPS measurements and data analysis.

REFERENCES

1. Topsøe, N-Y., and Topsøe, H., *J. Catal.* **139**, 631 (1993).
2. Prins, R., de Beer, V. H. J., and Somorjai, G. A., *Catal. Rev.-Sci. Eng.* **31**, 1 (1989).
3. Carvill, B. T., and Thompson, L. T., *Appl. Catal.* **75**, 249 (1991).
4. Topsøe, H., and Clausen, B. S., *Catal. Rev.-Sci. Eng.* **26**, 395 (1984).
5. Wivel, C., Candia, R., Clausen, B. S., Morup, S., and Topsøe, H., *J. Catal.* **68**, 453 (1981).
6. Daage, M., and Chianelli, R. R., *J. Catal.* **149**, 414 (1994).
7. Drew, M. G. B., Mitchell, P. C. H., and Kasztelan, S., *J. Chem. Soc. Farad. Trans.* **86**, 697 (1990).
8. Topsøe, N-Y., Topsøe, H., and Massoth, F. E., *J. Catal.* **119**, 252 (1989).
9. Harris, S., and Chianelli, R. R., *J. Catal.* **98**, 17 (1986).
10. Mitchell, P. C. H., *Catalysis (London)* **4**, 175 (1981).
11. Ekman, M. E., Anderegg, J. W., and Schrader, G. L., *J. Catal.* **117**, 246 (1989).
12. Delvaux, G., Grange, P., and Delmon, B., *J. Catal.* **56**, 99 (1979).
13. Alstrup, I., Chorkendorff, I., Candia, R., Clausen, B. S., and Topsøe, H., *J. Catal.* **77**, 397 (1982).
14. Voorhoeve, R. J. H., *J. Catal.* **23**, 236 (1971).
15. Konings, A. J. A., Valster, A., de Beer, V. H. J., and Prins, R., *J. Catal.* **76**, 466 (1982).
16. Thakur, D. S., and Delmon, B., *J. Catal.* **91**, 308 (1985).
17. Müller, B., van Langeveld, A. D., Moulijn, J. A., and Knözinger, H., *J. Phys. Chem.* **97**, 9028 (1993).
18. Weigand, B. C., and Friend, C. M., *Chem. Rev.* **92**, 491 (1992).
19. Angelici, R. J., *Bull. Soc. Chim. Belg.* **104**, 265 (1995).
20. McCarty, K. F., and Schrader, G. L., *Ind. Eng. Chem. Prod. Res. Dev.* **23**, 519 (1984).
21. Vasudevan, P. T., and Zhang, F., *Appl. Catal. A* **112**, 161 (1994).
22. Kasztelan, S., *Langmuir* **6**, 590 (1990).
23. Aigler, J. M., Kazansky, V. B., Houalla, M., Proctor, A., and Hercules, D. M., *J. Phys. Chem.* **99**, 11489 (1995).
24. Yermakov, Y. I., Kuznetsov, B. N., and Zakavov, V. A., "Catalysis by Supported Complexes." Elsevier, Amsterdam, 1981.
25. Aigler, J. M., Brito, J. L., Leach, P. A., Houalla, M., Proctor, A., Cooper, N. J., Hall, W. K., and Hercules, D. M., *J. Phys. Chem.* **97**, 5699 (1993).
26. Candlin, J. P., and Thomas, H., *Adv. Chem. Ser.* **132**, 212 (1974).
27. Sullivan, D. L., Roark, R. D., Ekerdt, J. G., Deutsch, S. E., and Gates, B. C., *J. Phys. Chem.* **99**, 3678 (1995).
28. Roark, R. D., Narayanan, C. R., Sullivan, D. L., and Ekerdt, J. G., *Chem. Mater.* **6**, 739 (1994).
29. Williams, C. C., Ekerdt, J. G., Jehng, J-M., Hardcastle, F. D., Turek, A. M., and Wachs, I. E., *J. Phys. Chem.* **95**, 8781 (1991).
30. Roark, R. D., Kohler, S. D., and Ekerdt, J. G., *Catal. Lett.* **16**, 71 (1992).
31. Roark, R. D., Kohler, S. D., Ekerdt, J. G., Kim, D. S., and Wachs, I. E., *Catal. Lett.* **16**, 77 (1992).
32. Williams, C. C., and Ekerdt, J. G., *J. Phys. Chem.* **97**, 6843 (1993).
33. Pollack, S. S., Makovsky, L. E., and Brown, F. R., *J. Catal.* **59**, 452 (1979).
34. Chastain (Ed.), "Handbook of X-ray Photoelectron Spectroscopy." Perkin–Elmer Corp., Eden Prairie, MN, 1992.
35. Yermakov, Yu. I., Startsev, A. N., and Burmistrov, V. A., *Appl. Catal.* **11**, 1 (1984).
36. Yermakov, Yu. I., Kuznetsov, B. N., Startsev, A. N., Burmistrov, V. A., Zhdan, P. A., Shepelin, A. P., and Zaikovaskii, V. I., *Kinet. and Catal.* **24**, 580 (1983).
37. Sullivan, D. L., and Ekerdt, J. G., unpublished results.
38. Owens, R. J., and Amberg, C. H., *Can. J. Chem.* **40**, 947 (1962).
39. Hensen, E. J. M., Vissenberg, M. J., de Beer, V. H. J., van Veen, J. A. R., and van Santen, R. A., *J. Catal.* **163**, 429 (1996).
40. Cotton, Wilkinson, and Gaus (Eds.), "Physical Chemistry," 2nd ed., p. 938. Freeman, New York, 1990.
41. Curtis, M. D., Penner-Hahn, J. E., Schwank, J., Baralt, O., McCabe, D. J., Thompson, L., and Waldo, G., *Polyhedron* **7**, 2411 (1988).
42. Kolboe, S., *Can. J. Chem.* **47**, 352 (1969).
43. Ihm, S-K., Moon, S-J., and Choi, H-J., *Ind. Eng. Chem. Res.* **29**, 1147 (1990).